Desalination and Water Treatment
www.deswater.com

doi: 10.5004/dwt.2023.29691

298 (2023) 222–232
June

Assessment of wave energy resources in the Pearl River estuary of China

Zuchao Ye, Xin Ma*, Na Yang, Liwei Cui

Beihai Marine Environmental Monitoring Center, State Oceanic Administration of China, Beihai 536000, China, email: oceanye2023@163.com

Received 18 December 2022; Accepted 19 May 2023

ABSTRACT

In the background of global carbon reduction, wave energy can provide a sustainable energy source in many coastal areas. Water depth is one of the factors that cannot be ignored in the assessment of wave energy resources, and the present study develops a new formula for evaluating wave energy suitable for any water depth. The availability wave energy around Wanshan of Guangdong, was analyzed for the past 20 y (2000–2020) using SWAN (simulating waves nearshore) model. This included an analysis of the annual and seasonal average distribution characteristics of wave energy. The 20 y of annual average data analysis showed that most of the significant wave height (H_s) was less than 1.2 m, and the annual average energy flux offshore can reach 4.0 kW/m. The available wave energy was most consistent in winter and least consistent in summer. The effective H_s occurred frequently, mostly over 50% of the year, in most of the research area except in the mouth of the Pearl River.

Keywords: Wanshan; Wave; Spatial-temporal variability; SWAN; Wave energy

1. Introduction

Energy needs and shortages have continued to grow in recent years, but environmental pollution caused by a lack of sufficient energy reserves and the excessive use of traditional fossil energy is becoming increasingly serious. Therefore, there is an urgent need to develop renewable energy technology designed to solve the shortcomings of and problems related to the use of traditional fossil energy [1]. Various kinds of renewable energy can replace traditional energy in many fields, helping to effectively alleviate the problem of insufficient reserves of traditional energy and to address environmental pollution. Among them, wave energy is considered the most likely alternative energy source that can be used to replace conventional energy in the next few decades [2]. Waves provide an energy resource with many advantages, such as the highest energy flux, limited negative impacts, and relatively high use factor [3–5]. A reasonable evaluation of the wave energy reserves in a study area is an important preparatory task that must be carried out before developing wave energy. Wave energy assessment for large-scale sea areas in different regions has been studied in many countries. In terms of the total global wave energy resources, the Climate Change Group (IPCC) believed that the total global wave energy resource was about 29,500 TWh/a, the technical exploitable capacity was about 500 GW, and its annual power generation was about 146 TWh/a. Some other studies believed that the total global wave energy resources were between 2,000 and 4,000 TWh/a [6–8].

The wave energy in the whole world had been evaluated to be in the range of 1–10 TW, which corresponds to the current level of energy demand globally [9]. So far, some studies on wave energy assessment have been conducted in different regions of the world, such as Argentina Portugal, Sweden, the US, China and other regions [10–25]. According to the global results given by Mørk et al. [26], the coasts of Europe's northernmost countries have one of the highest wave energy fluxes in the world, with a mean annual value of 70 kW/m [27,28]. China's wave energy reserves are not particularly abundant, although wave

* Corresponding author.

energy assessments have recently been conducted in some of China's waters. Regional studies can be conducted to analyze the wave energy reserves of an area more precisely and can be used to filter areas and identify those with a greater potential for development. Wave energy resources around Chinese sea could be systematically assessed using datasets calculated using the wave model Wave Watch III (WWIII) [24,25]. Liang et al. [29] and Wan et al. [30] also evaluated wave energy resources in different areas of China. In general, wave energy resources in the East China Sea are the most abundant, while those in the Bohai Sea are the least abundant. At the same time, scholars also analyzed the suitability of wave energy resources exploitation in China's sea, and generally concluded that China's sea is not an ideal area for wave energy exploitation.

When evaluating wave energy, calculating wave energy density is the key point. The current wave energy evaluation formula has a large error in the offshore area. Based on Eckart's work, Beji [31] and You [32] both proposed an explicit method for calculating the wave dispersion relation. For China, no high-precision assessment of wave energy resources around Wanshan has been carried out. This paper aims to assess wave energy around Wanshan area by adopting the equation proposed by You [32].

2. Wave energy estimation

According to the Shi et al. [33] and Liang et al. [34], the wave energy flux can be expressed as [31]:

$$P_w = \frac{1}{64\pi}\left[1+\frac{2kh}{\sinh(2kh)}\right]\rho g^2 H_s^2 T\tanh(kh) \tag{1}$$

where k is the wave number, h is water depth, ϱ is the seawater density, g is the gravity acceleration, H_s is the significant wave height and T is the energy period. The value of k can be obtained by $k = 2\pi/L$.

In most research, wave energy flux can be expressed [35,36]:

$$P = \frac{1}{64\pi}\rho g^2 H_s^2 T \tag{2}$$

Eq. (2) has been widely adopted to evaluate wave energy. In shallow and intermediate water, the influence of water depth is not considered and that will cause error when assess energy in these area [33]. We take λ as the ratio of Eq. (1) to Eq. (2) that can be expressed as Eq. (3). The variation trend of λ with water depth is shown in Fig. 1. Few researchers have noted that in shallow water and some water of intermediate depth, Eq. (2) overestimates wave energy, but for some other water of intermediate depth, Eq. (2) underestimates the available wave energy.

$$\lambda = \left[1+\frac{2kh}{\sinh(2kh)}\right]\tanh(kh) \tag{3}$$

In this paper, a new equation applicable at any water depth is compiled based on the explicit two-step wave diffusion equation proposed by You [32]. Compared to Eq. (2), the new equation has further improved its accuracy for estimating wave energy at any depth, especially in shallow water. The key to wave energy calculation is to obtain the exact kh value. The equation used to approximate kh was defined as:

$$kh \approx x_0 - \frac{f(x_0)}{f'(x_0)} = x_0\left[\frac{k_0 h + (x_0/\cosh x_0)^2}{x_0\tanh x_0 + (x_0/\cosh x_0)^2}\right] \tag{4}$$

where k_0 and x_0 are the deep-water wave number and is an initial estimate of kh, which can be calculated by Eq. (5):

$$\frac{x_0}{\sqrt{k_0 h}} \approx 1+\frac{1}{6}(k_0 h)+\frac{1}{30}(k_0 h)^2 \tag{5}$$

In this case, x_0 can be obtained by Eq. (5), and kh can be then obtained by Eq. (4), so the value of kh can be calculated by combining Eqs. (4) and (5) at any depth without cumbersome iteration. Wave energy can be assessed by combining Eqs. (1), (4), and (5).

3. Data

3.1. Research area and SWAN setting

The present study focused on the sea around Wanshan, administered by Zhuhai, Guangdong province of China. Zhuhai is adjacent to Macau and Hong Kong, and its economy is well developed. As an experimental sea area, wave energy resources needed to be assessed in this area. This paper only selected the region of 21.0–22.75°N, 112.5–115.5°E as the research area. Fish production is a very important industry for residents of Wanshan Island. Domestic and industrial activities, including fish production, require a massive amount of energy. According to the bathymetric dataset from the China Hydrographic Bureau, the average depth of the seas adjacent to Wanshan Island is considered to be approximately 17 m (Fig. 2).

SWAN model is normally applied to simulate the characteristics of waves [37,38]. The 360° of a circle were

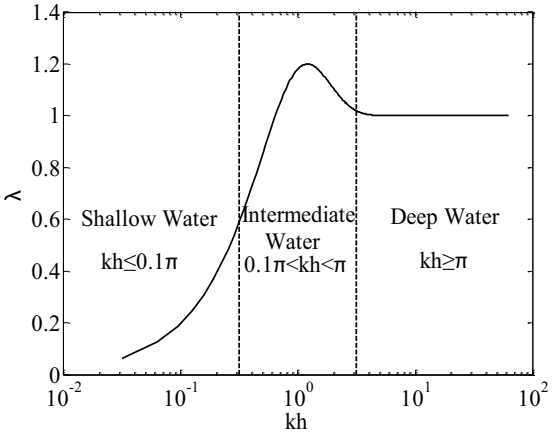

Fig. 1. Change in λ based on the change of kh.

divided into 36 equal areas of 10° each. Next, 24 bins for the frequency were obtained, and the minimum frequency was set to 0.04 Hz. The frequency used in this model was set to 1.1. In the model, we selected the option for exponential wind growth [39]. Wind fields were provided by ERA5 reanalysis datasets. The applicability of the ERA5 wind datasets to Chinese waters has been studied and shown to perform well [40]. To accurately obtain the boundary conditions of the incident waves, WWIII was used that covered the entire Chinese water. The model started in January 2001 and ended in December 2020, with the time step set to 1 h. The larger model has 0.1° × 0.1° grids, which are not described in this paper. For SWAN model, the model domain (Fig. 3) had a maximum area of 0.05° × 0.05° grids, with 30,164 grids and 58,324 nodes. There were 75 points on the open boundary, with a boundary scale of approximately 500 m. The grids in the nearshore area were refined, with a minimum grid scale of approximately 10 m. The calculation time step in SWAN was set to 2 min with the output time step set to 1 h.

3.2. Model validation

Wave data from three buoy stations, namely QF301, QF302, and QF303 (Fig. 3), were adopted to valid the model. Each station was located in deep water where the wave parameters have been recorded hourly for 20 y. A time series comparison between the measured H_s and the simulated records used for the validation was shown in Fig. 4. The results showed that the model can simulate well in focused area. We calculated the covariances of the three groups of data, which were 0.2038 (QF301), 0.2264 (QF302), and 0.1620 (QF303), indicating that the measured data of the three sites were positively correlated with the simulated data. In addition, some error metrics were adopted to quantitatively evaluate model. These included the relative error (δ) and correlation coefficient (R) in these three sites with 31.32%, 29.5%, and 28.1% for the relative errors and 0.86, 0.85, and 0.89 for the correlation coefficients, respectively. Based on relative error, the wave heights calculated using SWAN agreed with the buoy-recorded data well. The H_s correlation coefficients were found to be above 0.85 through the simulations, indicating that the model provided in this study can accurately simulate the wave parameters.

4. Results and discussion

4.1. Annual distribution of wave elements

The 20-y annual distribution of H_s, $\bar{T}$, and P_y were shown in Fig. 5a–c. Those (H_s, $\bar{T}$, and P_y) showed a gradual decreasing trend from deep water (offshore) to shallow water (nearshore). The average H_s was in the range of 0.2–1.2 m in most areas around Wanshan Islands and the maximum value occurred in the southern part of the study area. The $\bar{T}$ and P_y around Wanshan area were greater than 4 s and 5 kW/m in the same district, respectively.

The northeastern parts of the study area had greater wave height than that of the northwestern parts of the research area (Fig. 5c). Box plots of the annual mean values of the entire study area for H_s and P_y are shown in Fig. 6, from which the distribution of annual wave characteristics can be deeply understood.

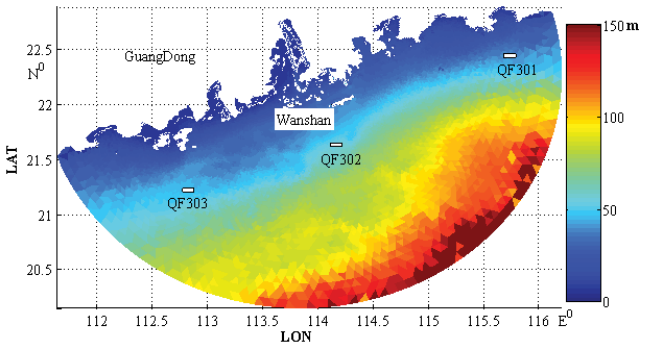

Fig. 2. Wanshan study area and the locations of observations at QF301, QF302, and QF303 along the coast of Guangdong, including Wanshan near Hong Kong.

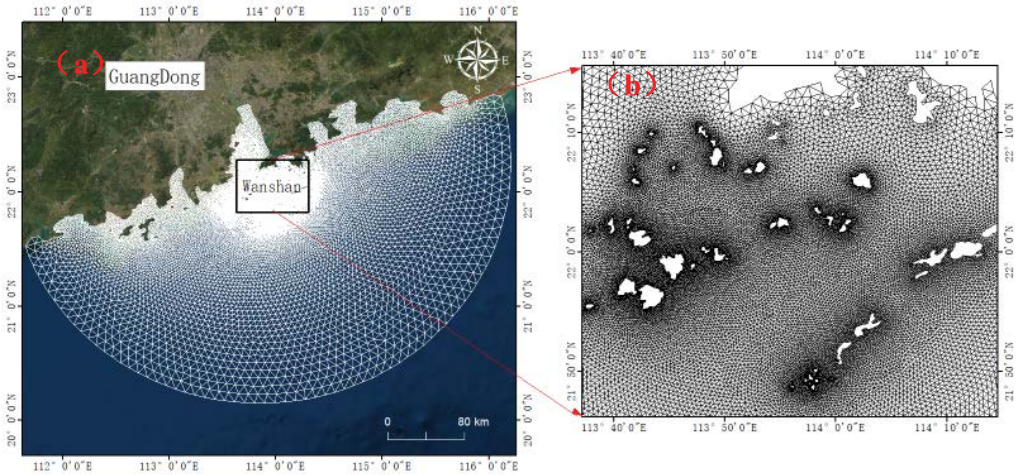

Fig. 3. Grid Settings for the computation area: (a) overview of the study area in general and (b) view of Wanshan area.

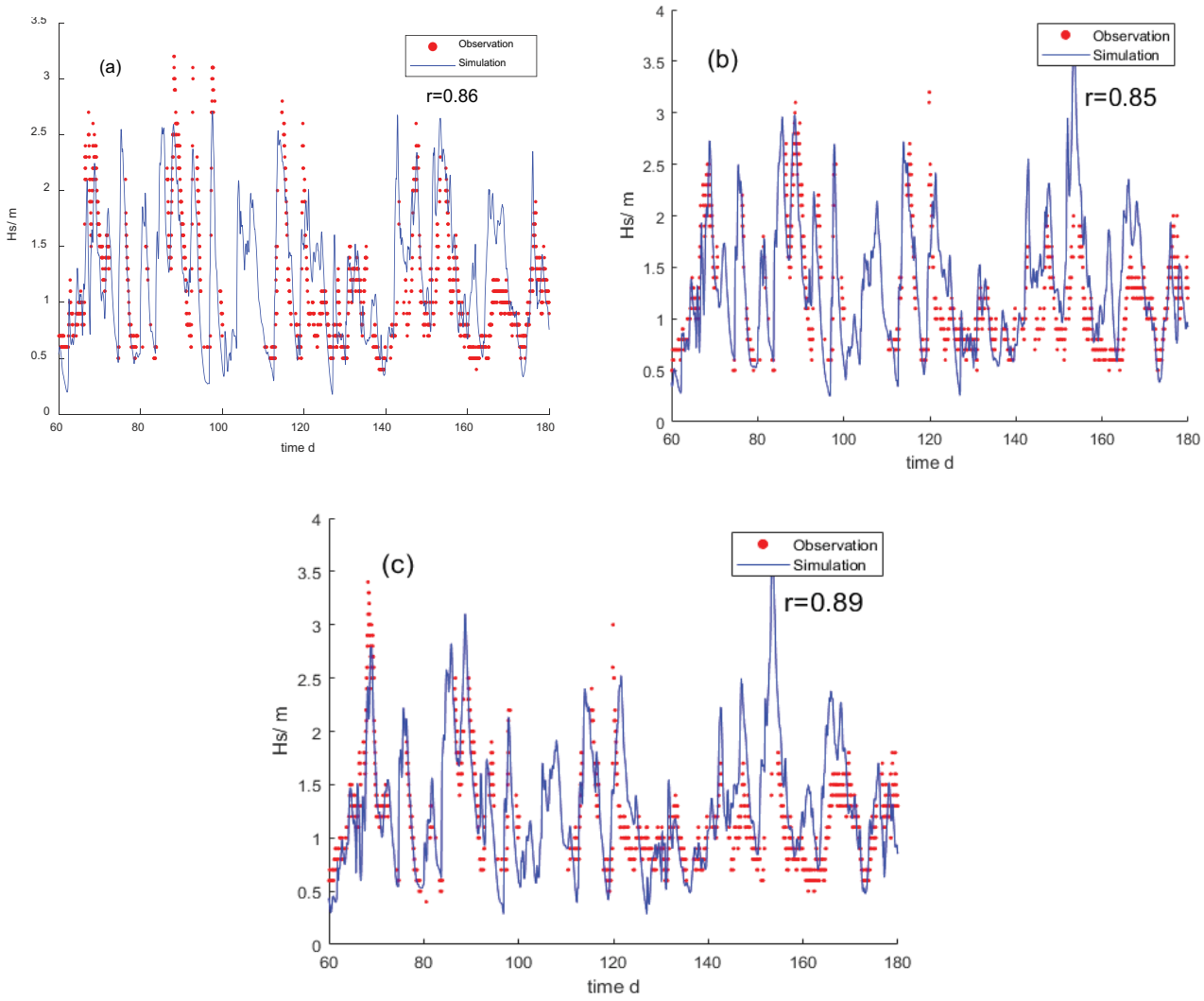

Fig. 4. Comparisons of the hindcasted H_s (red line) with the observational data (blue line) at: (a) QF301, (b) QF302, and (c) QF303.

The visual statistical factors such as minimum, median, and third quartiles can be provided by box plots for sample data [41]. For example, H_s and P_y did not change significantly year by year, with each parameter having considerable overlap from year to year; this indicates that H_s and P_y did not change significantly over time (Fig. 6). The average H_s was relatively low (less than 1.6 m) for the entire research period (2001–2020), while the average P_y was less than 11.5 kW/m. In the box diagram, a shorter or longer bar means the data discretization was lower or higher, respectively. Thus, the years with the higher data discretization for wave energy flux were 2003 and 2009. The years with the lowest and highest data discretization for wave energy were 2012 and 2009, respectively. The significant wave height fluctuated in a small range in any study year. The mean value of H_s was the smallest in 2012 and the largest in 2003.

4.2. Distribution of seasonal wave energy

The 20-y seasonal mean spatial distributions of H_s, $\overline{T}$, and P_y were presented in Figs. 8–10, respectively. The value of H_s peaked in winter (0.8–1.2 m) and reached the lowest values (0.5–0.7 m) in spring season in the research area (Fig. 7). That is, H_s was higher in winter and autumn seasons than that in other seasons. The $\overline{T}$ values in the four seasons ranged from 2–3 s around Wanshan Islands with little change over time (Fig. 8). Winter and spring had the highest and the lowest values of P_y, respectively, a pattern that was the same as those of H_s and $\overline{T}$ (Fig. 9). The P_y values peaked in winter and decreased in spring and then increased gradually in summer and autumn. Among them, a higher wave energy flux in winter was mainly distributed in the southeastern part of Wanshan Islands with values between 2.0 and 4.0 kW/m, while the wave energy flux in the northwestern part was lower with values of 0.5–2.0 kW/m.

The box plots of the seasonal means of H_s, $\overline{T}$ and P_y were presented in Fig. 10, which showed the seasons with the largest and least variations occurred in winter and spring, respectively. The box plots of H_s were shorter in spring compared to the other seasons indicating that the data were generally very consistent. The median (which

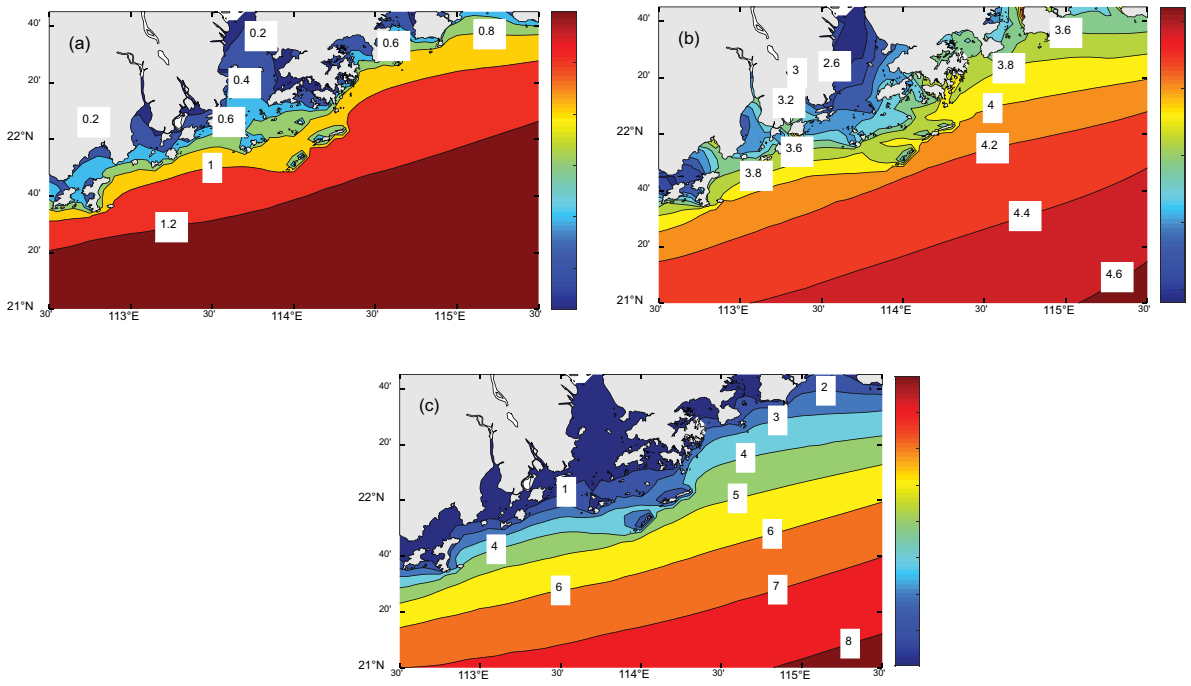

Fig. 5. The 20-y annual mean spatial distribution of H_s (a), $\overline{T}$ (b) and P_y (c).

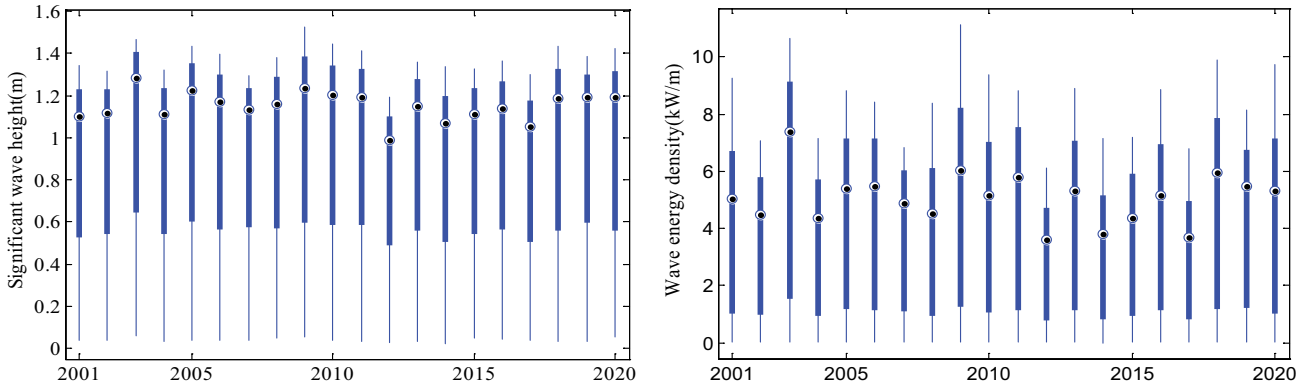

Fig. 6. Box plots of 20-y annual mean of the: H_s (a) and P_y (b) in the entire study area.

was generally close to the mean) gradually increased from spring to winter. The extreme variations of $\overline{T}$ occurred in the same seasons as those of H_s. However, the medians of the mean $\overline{T}$ had different distributions with $\overline{T}$ in summer being higher than that in autumn, and less than that in winter. The box plots of mean $\overline{T}$ are similar in the four seasons, indicating that $\overline{T}$ varied little in the four seasons. The extreme variations of P_y occurred in the same seasons as those of H_s and $\overline{T}$. However, the medians of P_y peaked in autumn, unlike those of H_s and $\overline{T}$.

4.3. Stability of wave resource

In past studies, the researchers thought that it was necessary to consider the stability of wave energy resources. Only stable wave energy resources can have real development value. The stability of P_y is related to wave energy conversion. The more stable it is, the more efficient the wave energy conversion will be; in addition, stable wave energy is beneficial to its full exploitation and use [42]. The efficiency of conversion will decrease as a result of discrete conditions. Therefore, we used to analyze the stability of wave energy. On this basis, the feasibility of developing wave energy resources was evaluated. The C_v is defined as:

$$C_v = \frac{S}{\overline{x}} \tag{6}$$

where $\overline{x}$ is the average H_s and P_y, and S is the standard deviation, C_v which can be expressed as:

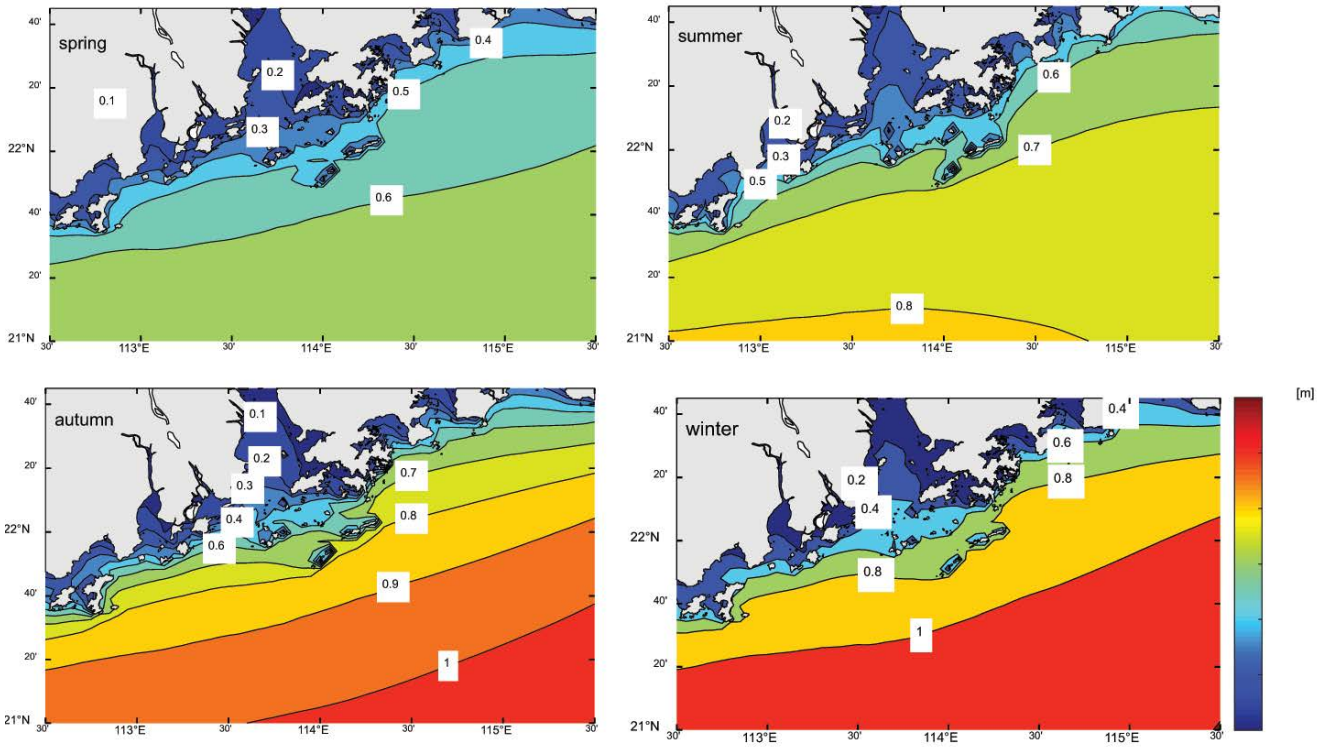

Fig. 7. Seasonal distribution of H_s around Wanshan area (unit: m).

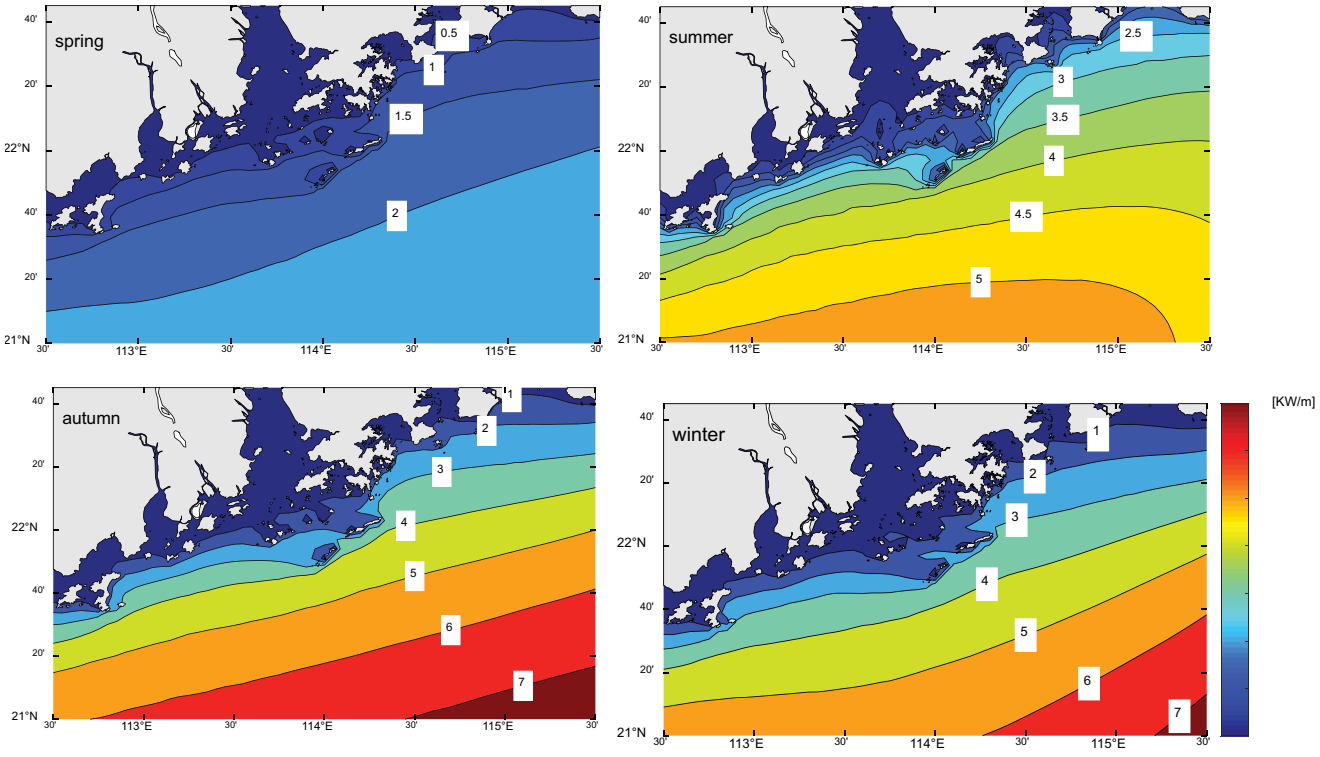

Fig. 8. Seasonal distribution of $\overline{T}$ around Wanshan area (unit: s).

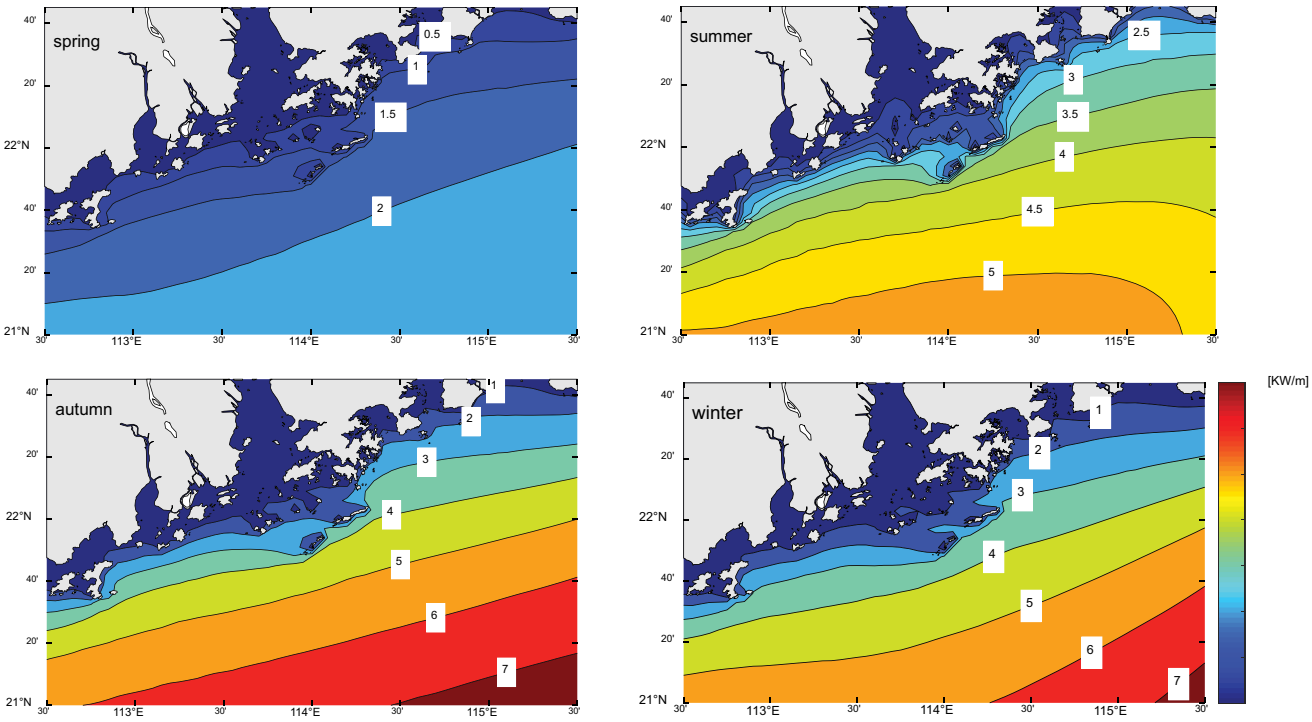

Fig. 9. Seasonal distribution of mean P_y around Wanshan area (unit: kW/m).

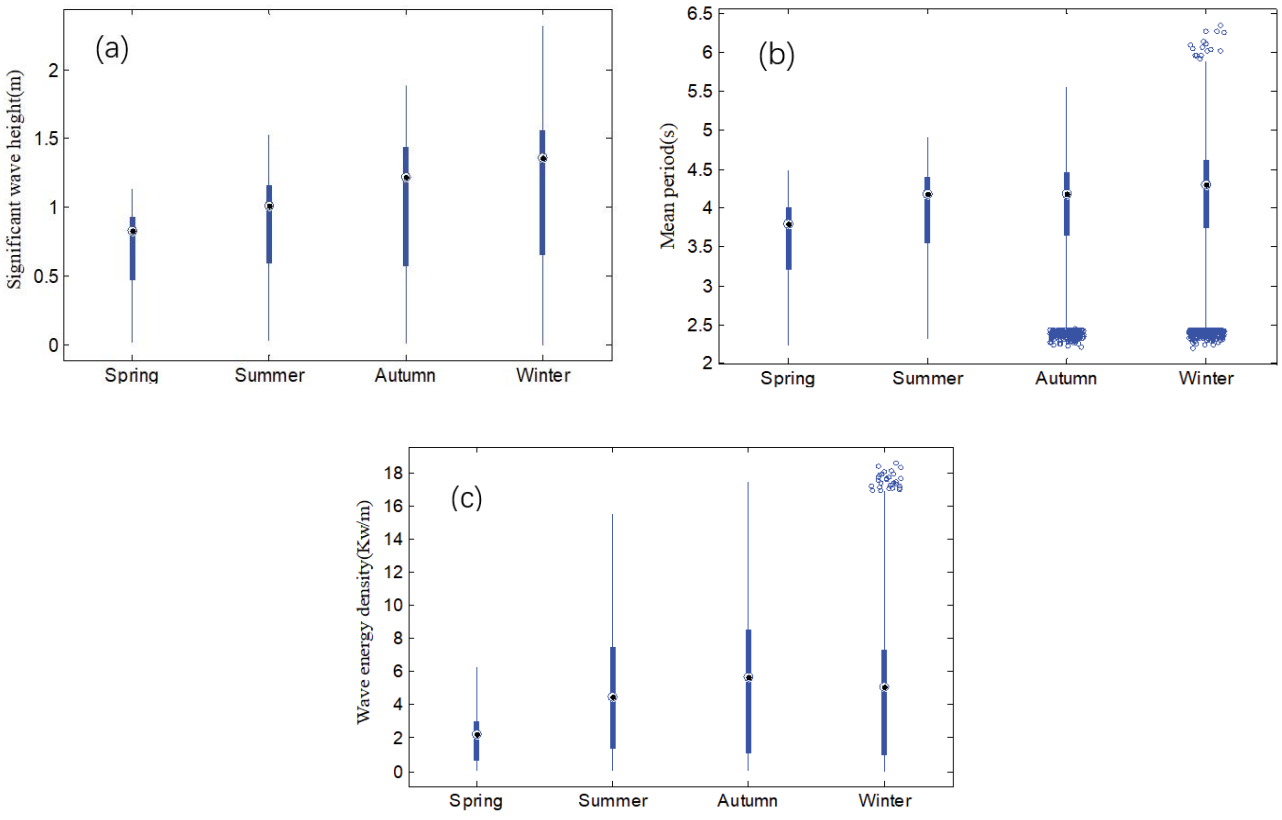

Fig. 10. Box plots of 20-y the seasonal means of: H_s (a), $\overline{T}$ (b) and P_y (c) in the study area.

$$S = \sqrt{\frac{\sum_{i=1}^{n} x_i^2 - \left(\sum_{i=1}^{n} x_i^2\right)/n}{n-1}} \tag{7}$$

The annual distribution of C_v for H_s and P_y are shown in Fig. 11. A smaller value of C_v, indicate smaller variability in the studied parameters. The nearshore regions had the highest C_v and it decreased toward the open sea (Fig. 11). This means that open sea areas are not only more energetic, but they can also provide more stable wave energy than nearshore area. Generally, for the area around Wanshan Islands, the highest temporal variability indices of H_s and P_y can be less than 1 and 2, respectively. It is interesting that the coefficient of dispersion (C_v) of H_s was less than that of P_y for the same points. The reason for this is that energy flux is a function of wave height squared, resulting in a higher rate of change.

The seasonal distribution of C_v for H_s and P_y is shown in Fig. 12. According to Fig. 12, generally for each studied season, C_v peaked in summer and was the smallest in winter. This means that Wanshan Sea experiences greater variation in wave energy in summer. The values of C_v for H_s in spring, summer, autumn, and winter were in the range of 1.5–2, 2.0–3.0, 1.5–2.0, and 0.5–1, respectively. In addition, the values of C_v around Wanshan Islands for wave flux in the same four seasons were in the range of 0.5–0.8, 0.5–1.0, 0.5–1.0, and 0–0.5, respectively. The above calculations reflect the low rate of change in P_y in winter and spring in the study area. It is interesting that: (1) although the P_y was lower in spring, it was more stable at the same time; (2) although the stability of H_s was poor in summer, the stability of P_y was more stable. In terms of the distribution and stability of P_y, winter is considered the best season for exploiting wave energy.

4.4. Frequency of effective H_s

As happens with any energy source, not all wave energy can be used by existing technology. By referring to current methods used in wind resources, this article introduced a new concept of the effective H_s in the wave energy resource assessment (short as H_{es}). Based on existing technology, waves between 0.5 m and 4.0 m can be captured by some equipment. In this paper, an H_s (0.5 m ≤ H_s ≤ 4.0 m) is regarded as the metric to decide whether the available wave could be used and is called H_{es}. It is important to note that H_{es} is a dynamic value that changes with technological innovation.

In the utilization of wave energy resources, the frequency of H_{es} in a region directly determines the development and utilization time of wave energy resources in this region. This paper analyzed the frequency of H_{es} over 20 y, using hourly wave data collected during Jan. 1, 2000 starting at 00:00 to Dec. 31, 2020 at 23:00. Fig. 13 showed the frequency of the H_{es} in research area was high, usually more than 50% except in the mouth of the Pearl River. As for Wanshan Islands, H_{es} ranged from 50%–70%, meaning that wave energy can be used here to generate electricity for than more than half of the time in a year.

4.5. Long-term linear trends of wave energy flux

The P_y at each node of the research area was averaged from 2001 to 2020, and the linear trend of P_y was analyzed over the last 20 a. In order to control the updating speed of variables and prevent the overall impact of sudden changes of variables, a five-point weighted moving average was adopted as shown in Eq. (8):

$$Y_i = \frac{X_{i-2} + 2X_{i-2} + 4X_i + 2X_{i+1} + X_{i+2}}{10} \qquad i = 2,3,\cdots,N-2 \tag{8}$$

where Y_i is the target value and the X_i is the original value. This method will fully reflect the trend of wave resources in different areas, helping researchers to avoid the disadvantages of deriving the data from the method of obtaining the trend by adopting the average value of the entire region.

The characteristics of the linear trend of the H_s are shown in Fig. 14a. During the last 20a, the H_s in most of the research area showed a slightly decreasing trend, with the ratio ranging from −0.005 to 0 m/a. The ratio was positive only in the northeastern area, indicating an increasing trend for H_s.

The characteristics of the linear trend of the P_y are shown in Fig. 14b. During the last 20a, P_y in all of the research area showed a decreasing trend year by year. Its distribution was different from the distribution of the significant wave height, even though they both tended to decrease. The zones with strongly decreasing trends were located in the southwestern waters (approx. −0.06 to −0.8 kW/(m·a)). The nearshore area showed weakly decreasing tendency for P_y (approx. −0.01 to 0 kW/(m·a)).

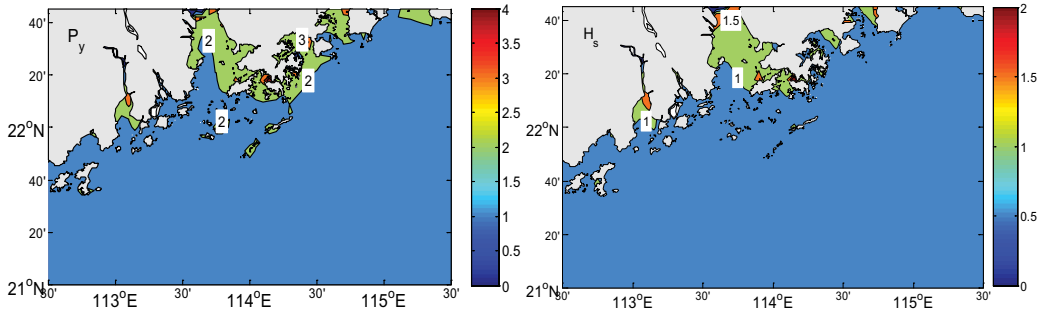

Fig. 11. Annual distribution of: (a) coefficient of dispersion (C_v) for P_y and (b) H_s.

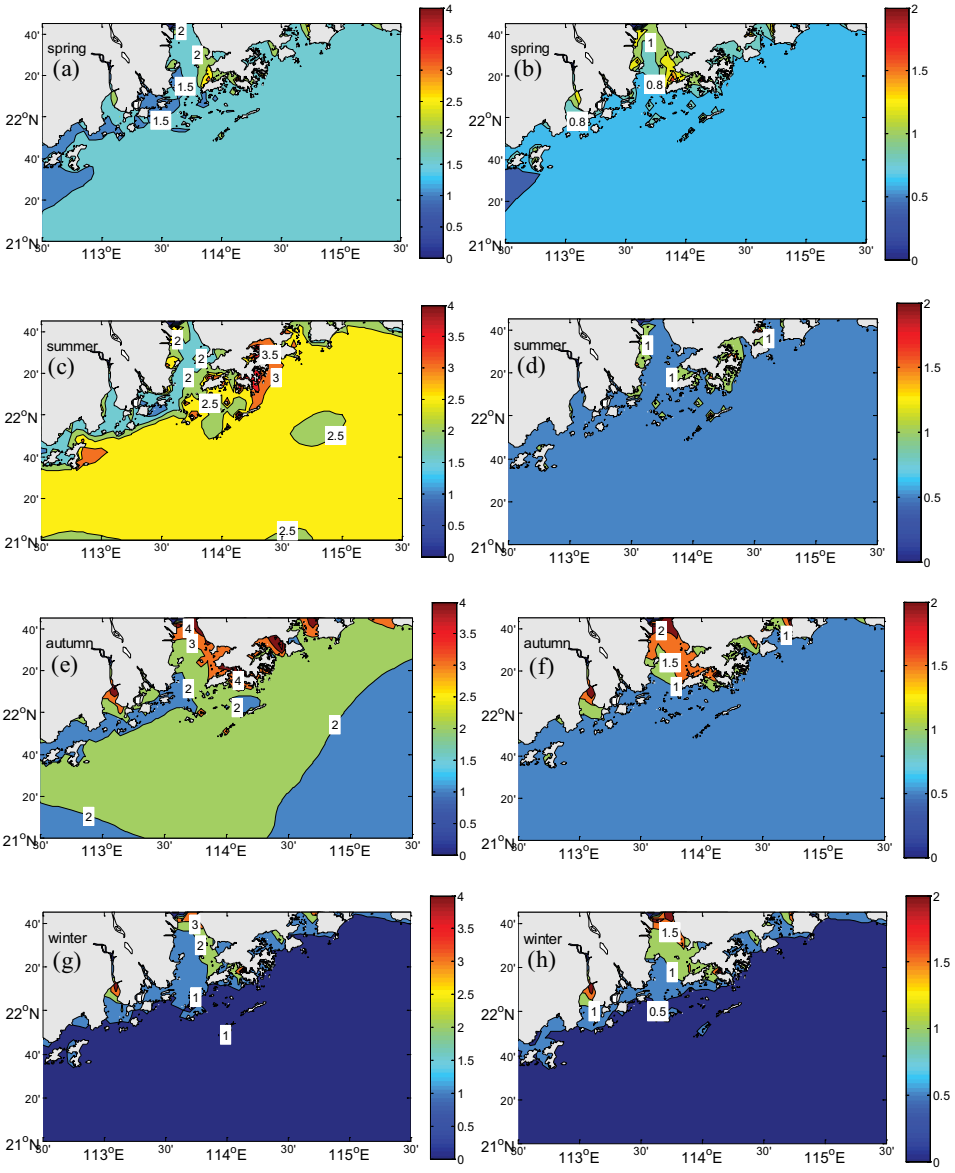

Fig. 12. Seasonal distribution of C_v for P_y (left) and H_s (right) in study sea area for: (a,b) spring, (c,d) summer, (e,f) autumn, and (g,h) winter.

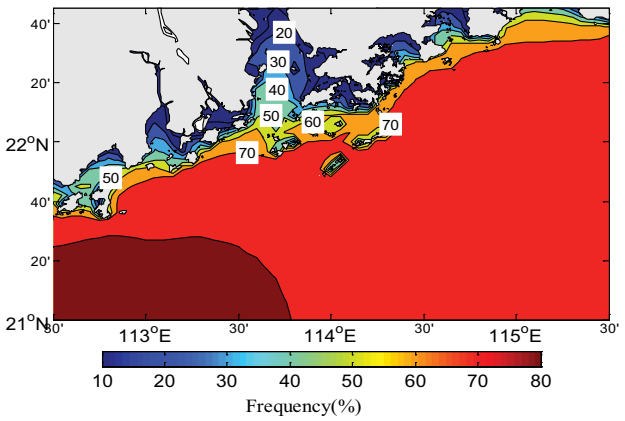

Fig. 13. Frequency of effective H_s over the 20-y study period.

4.6. Wave energy resource classification

In order to make better use of wave energy resources, it's necessary to classify wave energy resources in research area. But a common standard for the wave energy classification has not yet formed. Most previous studies have been based on P_y to determine suitability for development, such as 2 and 20 kW/m are defined as available and abundant watershed, respectively [43]. This paper established a simple system that suitable for research area (Table 1), and 4 grades were divided (Fig. 15). From Fig. 15, the wave energy resources around Wanshan Islands basically belonged to grade 2 level except the nearshore area. In the study area, most of the nearshore area belong to grade 1, with the exception of the northeastern area, which belong to grade 2. Unfortunately, the grades in studied

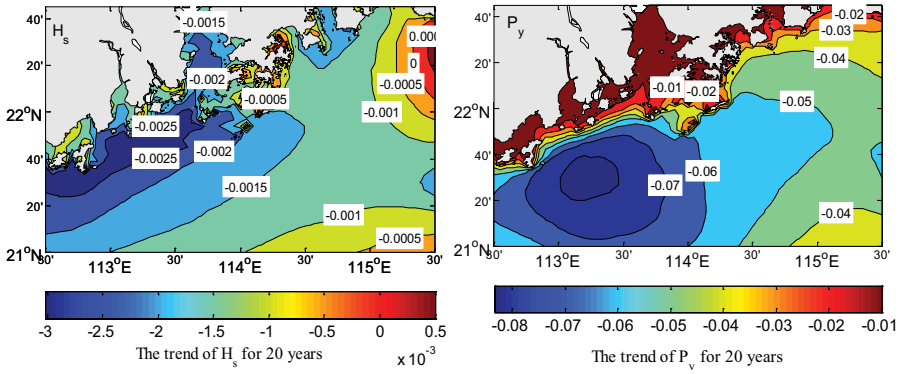

Fig. 14. Linear trends of (a) H_s and (b) P_y for the 20-y study period.

Table 1
Criteria for wave energy resource division

Grade	Annual average wave height (m)	Annual average wave energy flux (kW/m)	Annual hours of effective SWH (0.5~4 m)/h	Wave energy regionalized
1	0–0.5	<1	<4,000	Indigent area
2	0.5–1.5	1–5	4,000–6,000	Available area
3	1.5–2.5	5–20	6,000–8,000	Sub-rich area
4	>2.5	>20	>8,000	Rich area

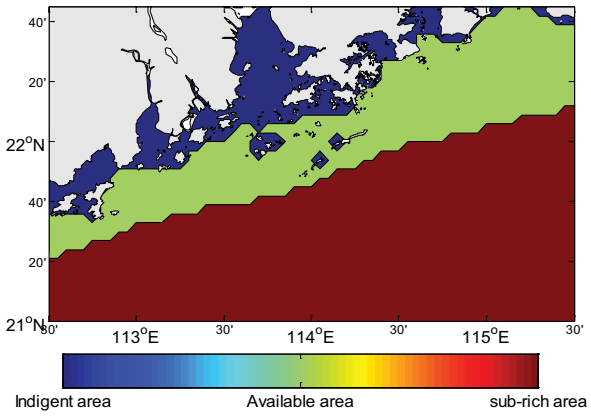

Fig. 15. Wave energy resource division in studied area.

area are all below level 4, and it proves that the resource condition is not very abundant for development.

5. Conclusion

During the research period (2001–2020), the annual average value of mean H_s was below 1.6 m, and P_y was less than 11.5 kW/m. The years with the larger variation for wave energy flux were 2003 and 2009. The largest range of wave energy flux occurred in 2009 and the smallest occurred in 2012. As for H_s, all the studies years had the similar range. The mean H_s in the year 2012 had the smallest, while the year 2003 had the largest.

The higher wave energy in winter was mainly distributed in southeastern part of the Wanshan Islands with a flux of 2.0–4.0 kW/m, while it is lower in the northwestern part with a flux of 0.5–2.0 kW/m. Maximum and minimum variations of H_s and P_y were presented in winter and spring, respectively. The H_s box plot was shorter in spring compared to the other seasons. This indicated that datasets in spring had a high consistency compared to those in other seasons. However, the medians of P_y in autumn was the highest, that was difference compared to H_s and T.

The nearshore regions had the highest C_v and it decreases towards the open sea. It means that open sea parts were not only energetic, but also more stable. Seasonal C_v statistics of wave energy showed that the wave energy in winter was the most stable and that in summer was the most unstable, respectively.

The frequency of H_{es} in most of the research area except Pearl River mouth is very high, mostly more than 50%. As for Wanshan Islands, it ranges from 50%–70%. That means than more than half of the time in a year can generate electricity.

During the nearly 20a, the P_y in all of the research area showed a decreasing trend. Its distribution was different from the distribution of the significant wave height, even though they both tended to decrease. The zones with high decreasing tendency were located in the southwestern waters (about –0.06~–0.8 kW/(m·a)). The nearshore area showed low decreasing tendency (about –0.01~0 kW/(m·a)).

In the study area, most of the nearshore area belonged to grade 1, with the exception of the northeastern area, which belonged to grade 2. Unfortunately, the grades in studied area were all below level 4, and there is no rich region for wave development. Although there is no optimal area for wave energy utilization in Wanshan Sea area, this paper proposes a wave energy evaluation method based

on EWSH and the duration of it and the stability of wave energy, which is also applicable to other sea areas.

References

[1] K. Mahmoodi, H. Ghassemi, A. Razminia, Temporal and spatial characteristics of wave energy in the Persian Gulf based on the ERA5 reanalysis dataset, Energy, 187 (2019) 115991, doi: 10.1016/j.energy.2019.115991.

[2] G. Iglesias, R. Carballo, Wave energy potential along the Death Coast (Spain), Energy, 34 (2009) 1963–1975.

[3] A. Clément, P. McCullen, A. Falcão, A. Fiorentino, F. Gardner, K. Hammarlund, G. Lemonis, T. Lewis, K. Nielsen, S. Petroncini, M.-Teresa Pontes, P. Schild, B.-O. Sjöström, H.C. Sørensen, T. Thorpe, Wave energy in Europe: current status and perspectives, Renewable Sustainable Energy Rev., 6 (2002) 405–431.

[4] M. Leijon, H. Bernhoff, M. Berg, O. Ågren, Economical considerations of renewable electric energy production—especially development of wave energy, Renewable Energy, 8 (2003) 1201–1209.

[5] U. Henfridsson, V. Neimane, K. Strand, R. Kapper, H. Bernhoff, O. Danielsson, M. Leijon, J. Sundberg, K. Thorburn, E. Ericsson, K. Bergman, Wave energy potential in the Baltic Sea and the Danish part of the North Sea, with reflections on the Skagerrak, Renewable Energy, 32 (2007) 2069–2084.

[6] J. Cruz, Ocean Wave Energy, Springer Berlin, Heidelberg, 2008.

[7] A.F. de O. Falcão, Wave energy utilization: a review of the technologies, Renewable Sustainable Energy Rev., 14 (2010) 899–918.

[8] M. Kadiri, R. Ahmadian, B. Bockelmann-Evans, W. Rauen, R. Falconer, A review of the potential water quality impacts of tidal renewable energy systems, Renewable Sustainable Energy Rev., 16 (2012) 329–341.

[9] N.N. Panicker, Power resource estimate of ocean surface waves, Ocean Eng., 3 (1976) 429–439.

[10] N.W. Lanfredi, J.L. Pousa, C.A. Mazio, W.C. Dragani, Wave-power potential along the coast of the province of Buenos Aires, Argentina, Energy, 17 (1992) 997–1006.

[11] M.T. Pontes, R. Aguiar, H. Oliveira Pires, A nearshore wave energy atlas for Portugal, J. Offshore Mech. Arct. Eng., 127 (2005) 249–255.

[12] E. Rusu, C. Guedes Soares, Numerical modelling to estimate the spatial distribution of the wave energy in the Portuguese nearshore, Renewable Energy, 34 (2009) 1501–1516.

[13] H. Bernhoff, E. Sjöstedt, M. Leijon, Wave energy resources in sheltered sea areas: a case study of the Baltic Sea, Renewable Energy, 31 (2006) 2164–2170.

[14] R. Waters, J. Engström, J. Isberg, M. Leijon, Wave climate off the Swedish west coast, Renewable Energy, 34 (2009) 1600–1606.

[15] J.H. Wilson, A. Beyene, California wave energy resource evaluation, J. Coastal Res., 23 (2007) 679–690.

[16] J.E. Stopa, K.F. Cheung, Y.-L. Chen, Assessment of wave energy resources in Hawaii, Renewable Energy, 36 (2011) 554–567.

[17] C.W. Zheng, C.Y. Li, J. Pan, M.Y. Liu, L.L. Xia, An overview of global ocean wind energy resource evaluations, Renewable Sustainable Energy Rev., 53 (2016) 1240–1251.

[18] C.-w. Zheng, J. Pan, J.-x. Li, Assessing the China Sea wind energy and wave energy resources from 1988 to 2009, Ocean Eng., 65 (2013) 39–48.

[19] C.W. Zheng, L.T. Shao, W.L. Shi, Q. Su, G. Lin, X.Q. Li, X.B. Chen, An assessment of global ocean wave energy resources over the last 45 a, Acta Oceanolog. Sin., 33 (2014) 92–101.

[20] M. Folley, T.J.T. Whittaker, Analysis of the nearshore wave energy resource, Renewable Energy, 34 (2009) 1709–1715.

[21] F. Chen, S.-M. Lu, K.-T. Tseng, S.-C. Lee, E. Wang, Assessment of renewable energy reserves in Taiwan, Renewable Sustainable Energy Rev., 14 (2010) 2511–2528.

[22] M.G. Hughes, A.D. Heap, National-scale wave energy resource assessment for Australia, Renewable Energy, 35 (2010) 1783–1791.

[23] G. Iglesias, R. Carballo, Wave energy resource in the Estaca de Bares area (Spain), Renewable Energy, 35 (2010) 1574–1584.

[24] G.W. Kim, W.M. Jeong, K.S. Lee, K.C. Jun, M.E. Lee, Offshore and nearshore wave energy assessment around the Korean Peninsula, Energy, 36 (2011) 1460–1469.

[25] A. Akpınar, M. Ihsan Kömürcü, Assessment of wave energy resource of the Black Sea based on 15-year numerical hindcast data, Appl. Energy, 101 (2013) 502–512.

[26] G. Mørk, S. Barstow, A.K. Kabuth, M. Teresa Pontes, Assessing the Global Wave Energy Potential, Proceedings of OMAE2010 29th International Conference on Ocean, Offshore Mechanics and Arctic Engineering, Shanghai, China, 2010, pp. 6–11.

[27] D. Mollison, Wave Climate and the Wave Power Resource, D.V. Evans, A.F.O. de Falcão, Eds., Hydrodynamics of Ocean Wave-Energy Utilization, International Union of Theoretical and Applied Mechanics, Springer, Berlin, Heidelberg, 1986, pp. 133–156.

[28] M.T. Pontes, Assessing the European wave energy resource, J. Offshore Mech. Arct. Eng., 120 (1998) 226–231.

[29] B.C. Liang, F. Fan, F.S. Liu, S.H. Gao, H.Y. Zuo, 22-Year wave energy hindcast for the China East Adjacent Seas, Renewable Energy, 71 (2014) 200–207.

[30] Y. Wan, C.Q. Fan, J. Zhang, J.M. Meng, Y.S. Dai, L.G. Li, W.F. Sun, P. Zhou, J. Wang, X.D. Zhang, Wave energy resource assessment off the coast of China around the Zhoushan Islands, Energies, 10 (2017) 1320, doi: 10.3390/en10091320.

[31] S. Beji, Improved explicit approximation of linear dispersion relationship for gravity waves, Coastal Eng., 73 (2013) 11–12.

[32] Z.-J. You, A close approximation of wave dispersion relation for direct calculation of wavelength in any coastal water depth, Appl. Ocean Res., 30 (2008) 113–119.

[33] H.Y. Shi, X.R. Zhang, W.Y. Du, Q.J. Li, H.L. Qu, Z.J. You, Assessment of wave energy resources in China, J. Mar. Sci. Eng., 10 (2022) 1771, doi: 10.3390/jmse10111771.

[34] B.C. Liang, Z.X. Shao, G.X. Wu, M. Shao, J.W. Sun, New equations of wave energy assessment accounting for the water depth, Appl. Energy, 188 (2017) 130–139.

[35] D. Myrhaug, B.J. Leira, H. Holm, Wave power statistics for individual waves, Appl. Ocean Res., 31 (2009) 246–250.

[36] A.H. Izadparast, J.M. Niedzwecki, Estimating the potential of ocean wave power resources, Ocean Eng., 38 (2011) 177–185.

[37] N. Booij, R.C. Ris, L.H. Holthuijsen, A third-generation wave model for coastal regions: 1. Model description and validation, J. Geophys. Res., 104 (1999) 7649–7666.

[38] R.C. Ris, L.H. Holthuijsen, N. Booij, A third-generation wave model for coastal regions: 2. Verification, J. Geophys. Res., 104 (1999) 7667–7681.

[39] P.A.E.M. Janssen, Quasi-linear theory of wind-wave generation applied to wave forecasting, J. Phys. Oceanogr., 21 (1991) 1631–1642.

[40] H.Y. Shi, X.F. Cao, Q.J. Li, D.L. Li, J.C. Sun, Z.J. You, Q.Y. Sun, Evaluating the accuracy of ERA5 wave reanalysis in the water around China, J. Ocean Univ. China, 20 (2021) 1–9.

[41] M. Vaghefi, K. Mahmoodi, M. Akbari, A comparison among data mining algorithms for outlier detection using flow pattern experiments, Sci. Iran., 25 (2018) 590–605.

[42] A.M. Cornett, A Global Wave Energy Resource Assessment, Proceedings of the Eighteenth International Offshore and Polar Engineering, The International Society of Offshore and Polar Engineers, Conference Held in Canada, Vancouver, 2008, pp. 318–326.

[43] M. Gonçalves, P. Martinho, C. Guedes Soares, Wave energy assessment based on a 33-year hindcast for the Canary Islands, Renewable Energy, 152 (2020) 259–269.